REPORT DOCUMENTATION PAGE

Form Approved OMB NO. 0704-0188

1. REPORT DATE (DD-MM-YYYY)	2. REPORT TYPE	3. DATES COVERED (From - To)
28-02-2017	Final Report	1-Sep-2015 - 31-Aug-2019

4. TITLE AND SUBTITLE
Final Report: Electrically Injected 280 nm AlGaN Nanowire Lasers on Silicon

5a. CONTRACT NUMBER
W911NF-15-1-0168

5b. GRANT NUMBER

5c. PROGRAM ELEMENT NUMBER
611102

6. AUTHORS
Zetian Mi

5d. PROJECT NUMBER

5e. TASK NUMBER

5f. WORK UNIT NUMBER

7. PERFORMING ORGANIZATION NAMES AND ADDRESSES
McGill University
845 Sherbrooke Street West, 2nd Floor

8. PERFORMING ORGANIZATION REPORT NUMBER

9. SPONSORING/MONITORING AGENCY NAME(S) AND ADDRESS (ES)
U.S. Army Research Office
P.O. Box 12211
Research Triangle Park, NC 27709-2211

10. SPONSOR/MONITOR'S ACRONYM(S)
ARO

11. SPONSOR/MONITOR'S REPORT NUMBER(S)
67075-EL.9

12. DISTRIBUTION AVAILIBILITY STATEMENT
Approved for Public Release; Distribution Unlimited

13. SUPPLEMENTARY NOTES
The views, opinions and/or findings contained in this report are those of the author(s) and should not contrued as an official Department of the Army position, policy or decision, unless so designated by other documentation.

14. ABSTRACT
To date, the performance of deep UV optoelectronic devices has been limited by the presence of extremely large densities of threading dislocations, strong polarization field and the related quantum-confined Stark effect, and extremely poor p-type conduction of AlN. We have recently demonstrated that the afore-described challenges for achieving high performance deep UV optoelectronic devices can be fundamentally addressed by the emerging AlGaN nanowire structures. We have performed a detailed investigation of the molecular beam epitaxial growth and characterization of Al-rich AlGaN nanowire heterostructures. We have discovered that AlGaN quantum dot

15. SUBJECT TERMS
AlGaN, nanowire, laser

16. SECURITY CLASSIFICATION OF:			17. LIMITATION OF ABSTRACT	15. NUMBER OF PAGES	19a. NAME OF RESPONSIBLE PERSON
a. REPORT	b. ABSTRACT	c. THIS PAGE			Zetian Mi
UU	UU	UU	UU		19b. TELEPHONE NUMBER +15-143-9871

Report Title

Final Report: Electrically Injected 280 nm AlGaN Nanowire Lasers on Silicon

ABSTRACT

To date, the performance of deep UV optoelectronic devices has been limited by the presence of extremely large densities of threading dislocations, strong polarization field and the related quantum-confined Stark effect, and extremely poor p-type conduction of AlN. We have recently demonstrated that the afore-described challenges for achieving high performance deep UV optoelectronic devices can be fundamentally addressed by the emerging AlGaN nanowire structures. We have performed a detailed investigation of the molecular beam epitaxial growth and characterization of Al-rich AlGaN nanowire heterostructures. We have discovered that AlGaN quantum dot-like nanostructures can be spontaneously formed in nearly defect-free AlGaN nanowire structures, which can provide superior three-dimensional quantum-confinement of charge carriers and drastically reduce the transparent carrier density compared to conventional quantum wells. Moreover, both Si and Mg dopant incorporation can be significantly enhanced in nanowire structures, due to the much reduced formation energy in nanowires, thereby leading to highly efficient current conduction that was not previously possible. We have further demonstrated, for the first time, electrically pumped AlGaN nanowire lasers operating in the UV-B and UV-C bands.

Enter List of papers submitted or published that acknowledge ARO support from the start of the project to the date of this printing. List the papers, including journal references, in the following categories:

(a) Papers published in peer-reviewed journals (N/A for none)

Received		Paper
02/28/2017	1	Ashfiqua Tahseen Connie, Songrui Zhao, Sharif Md. Sadaf, Ishiang Shih, Zetian Mi, Xiaozhang Du, Jingyu Lin, Hongxing Jiang. Optical and electrical properties of Mg-doped AlN nanowires grown by molecular beam epitaxy, Applied Physics Letters, ( ): 213105. doi:
02/28/2017	2	S. Zhao, M. Djavid, Z. Mi. Surface Emitting, High Efficiency Near-Vacuum Ultraviolet Light Source with Aluminum Nitride Nanowires Monolithically Grown on Silicon, Nano Letters, ( ): 7006. doi:
02/28/2017	4	Binh H. Le, Songrui Zhao, Xianhe Liu, Steffi Y. Woo, Gianluigi A. Botton, Zetian Mi. Controlled Coalescence of AlGaN Nanowire Arrays: An Architecture for Nearly Dislocation-Free Planar Ultraviolet Photonic Device Applications, Advanced Materials, ( ): 8446. doi:
02/28/2017	3	S. Zhao, S. Y. Woo, M. Bugnet, X. Liu, J. Kang, G. A. Botton, Z. Mi. Three-Dimensional Quantum Confinement of Charge Carriers in Self-Organized AlGaN Nanowires: A Viable Route to Electrically Injected Deep Ultraviolet Lasers, Nano Letters, ( ): 7801. doi:
02/28/2017	5	S. Zhao, X. Liu, Y. Wu, Z. Mi. An electrically pumped 239 nm AlGaN nanowire laser operating at room temperature, Applied Physics Letters, ( ): 191106. doi:
02/28/2017	6	S. Zhao, S. M. Sadaf, S. Vanka, Y. Wang, R. Rashid, Z. Mi. Sub-milliwatt AlGaN nanowire tunnel junction deep ultraviolet light emitting diodes on silicon operating at 242 nm, Applied Physics Letters, ( ): 201106. doi:
02/28/2017	7	S. M. Sadaf, S. Zhao, Y. Wu, Y.-H. Ra, X. Liu, S. Vanka, Z. Mi. An AlGaN Core–Shell Tunnel Junction Nanowire Light-Emitting Diode Operating in the Ultraviolet-C Band, Nano Letters, ( ): 1212. doi:
02/28/2017	8	Nhung Hong Tran, Binh Huy Le, Songrui Zhao, Zetian Mi. On the mechanism of highly efficient p-type conduction of Mg-doped ultra-wide-bandgap AlN nanostructures, Applied Physics Letters, ( ): 032102. doi:
TOTAL:	**8**	

Number of Papers published in peer-reviewed journals:

(b) Papers published in non-peer-reviewed journals (N/A for none)

Received	Paper

TOTAL:

Number of Papers published in non peer-reviewed journals:

(c) Presentations

1. (Invited) S. Zhao, X. Liu, and Z. Mi, "Electrically injected AlGaN nanowire deep ultraviolet lasers on Si," SPIE Photonics West, San Francisco, CA, Jan. 30-Feb. 2, 2017.
2. (Invited) Z. Mi, S. Zhao, and S. Sadaf, "AlGaN nanowire light emitting diodes: Breaking the efficiency bottleneck of deep ultraviolet light sources," SPIE Photonics West, San Francisco, CA, Jan. 30-Feb. 2, 2017.
3. (Keynote) Z. Mi, "Emerging applications of III-nitride nanostructures: From deep UV photonics to artificial photosynthesis," UK Nitrides Consortium Conference, Oxford, UK, Jan. 5-6, 2017.
4. S. M. Sadaf, S. Zhao, Y. Wu, Y.-H. Ra, X. Liu, and Z. Mi, "Tunnel junction enhanced high power deep ultraviolet nanowire light emitting diodes," 32nd North American Molecular Beam Epitaxy Conference, Saratoga Springs, NY, Sept. 18-21, 2016.
5. S. Zhao, S. Sadaf, X. Liu, and Z. Mi, "Molecular beam epitaxial growth and characterization of AlGaN nanowires for 240 nm emitting UV LEDs and lasers," 32nd North American Molecular Beam Epitaxy Conference, Saratoga Springs, NY, Sept. 18-21, 2016.
6. (Invited) Z. Mi, S. Zhao, X. Liu, S. Y. Woo, M. Bugnet, and G. A. Botton, "Electrically injected AlGaN nanowire deep ultraviolet lasers," IEEE Photonics Conference, Waikoloa, Hawaii, Sept. 2-6, 2016.
7. S. Zhao, X. Liu, S. Y. Woo, Y. Wu, S. Sadaf, R. Rashid, Y. Wang, D. Laleyan, G. A. Botton, and Z. Mi, "AlGaN nanowire deep UV LEDs and lasers operating below 240 nm," International Workshop on Nitride Semiconductors, Orlando, FL, Oct. 2-7, 2016.
8. (Invited) Z. Mi, S. Zhao, X. Liu, S. Y. Woo, M. Bugnet, and G. A. Botton, "Al(Ga)N nanowire deep ultraviolet light emitting diodes and lasers," International Conference on Molecular Beam Epitaxy (ICMBE 2016), Montpellier, France, Sept. 4-9, 2016.
9. (Invited) Z. Mi and S. Zhao, "AlGaN nanowire deep ultraviolet LEDs and lasers," 2016 IEEE Summer Topical Meeting on Nanowire Optoelectronics, Newport Beach, CA, July 11-13, 2016.
10. (Invited) Z. Mi and S. Zhao, "Electrically Pumped Lasers and Light Emitting Diodes in the Ultraviolet-C Band with AlGaN Nanowires," 229th ECS Meeting, San Diego, CA, May 29 - June 3, 2016.
11. (Invited) Z. Mi, S. Zhao, X. Liu, S. Y. Woo, and G. A. Botton, "Electrically injected AlGaN nanowire deep ultraviolet lasers on Si", SPIE Photonics West (SPIE Photonics West 2016), San Francisco, California, United States, Feb. 2016.
12. S. Zhao, D. Laleyan, M. Djavid, B. H. Le, X. Liu, and Z. Mi, "A surface-emitting electrically-injected near vacuum ultraviolet light source with aluminum nitride nanowires", SPIE Photonics West (SPIE Photonics West 2016), San Francisco, California, United States, Feb. 2016.
13. (Keynote) Z. Mi, S. Zhao, X. Liu, B. H. Le, M. G. Kibria, F. A. Chowdhury, "Tuning the surface charge properties of III-nitride nanowires: From ultralow threshold deep UV lasers to high efficiency artificial photosynthesis", The 6th International Symposium on Growth of III-Nitrides (ISGN 2015), Hamamatsu, Japan, Nov. 2015.
14. N. H. Tran, S. Zhao, B. H. Le, and Z. Mi, "Impurity-band conduction in Mg-doped AlN nanowires", The 31th North American Molecular Beam Epitaxy Conference (NAMBE 2015), Mayan Riviera, Mexico, Oct. 2015.
15. B. H. Le, S. Zhao, X. Liu, Y. H. Ra, M. Djavid, and Z. Mi, "Electrically injected GaN/AlGaN nanowire ultraviolet lasers by selective area growth", The 31th North American Molecular Beam Epitaxy Conference (NAMBE 2015), Mayan Riviera, Mexico, Oct. 2015.
16. (Invited) Z. Mi, S. Zhao, X. Liu, K. H. Li, J. Kang, Q. Wang, S. Y. Woo, and G. Botton "Electrically injected AlGaN nanowire deep UV lasers on Si", 11th International Conference on Nitride Semiconductors (ICNS 2015), Beijing, China, Aug. 2015.
17. S. Zhao, A. T. Connie, M. H. T. Dastjerdi, S. Sadaf, I. Shih, and Z. Mi, "Molecular beam epitaxial growth and characterization of AlN nanowire LEDs on Si", 11th International Conference on Nitride Semiconductors (ICNS 2015), Beijing, China, Aug. 2015.
18. S. Zhao, X. Liu, K.-H. Li, S. Y. Woo, G. Botton, and Z. Mi, "AlGaN nanowire ultraviolet lasers on Si", 2015 IEEE Summer Topicals Meeting Series (SUM-IEEE 2015), Nassau, Bahamas, Jul. 2015.
19. S. Zhao, A. T. Connie, B. H. Le, X. H. Kong, H. Guo, X. Z. Du, J. Y. Lin, H. X. Jiang, I. Shih, and Z. Mi, "p-Type AlN nanowires and AlN nanowire light emitting diodes on Si", 2015 IEEE Summer Topicals Meeting Series (SUM-IEEE 2015), Nassau, Bahamas, Jul. 2015.
20. S. Zhao, A. T. Connie, B. H. Le, I. Shih, and Z. Mi, "Molecular beam epitaxial growth and characterization of AlN nanowire LEDs: Breaking the bottleneck of deep UV light sources," 2015 Compound Semiconductor Week (CSW 2015), University of California, Santa Barbara, California, United States, Jul. 2015.
21. S. Zhao, X. Liu, B. H. Le, J. J. Kang, K. H. Li, Q. Wang, and Z. Mi, "Electrically injected deep ultraviolet lasers based on AlGaN nanostructures," 2015 Compound Semiconductor Week (CSW 2015), University of California, Santa Barbara, California, United States, Jul. 2015.
22. S. Zhao, X. Liu, J. J. Kang, K. H. Li, Q. Wang, and Z. Mi, "Electrically injected AlGaN nanowire ultraviolet lasers," 57th Electronic Materials Conference (EMC 2015), The Ohio State University, Columbus, Ohio, Jun. 2015.
23. S. Zhao, A. T. Connie, M. H. T. Dasterjdi, S. Sadaf, I. Shih, and Z. Mi, "Molecular beam epitaxial growth and characterization of AlN nanowire LEDs on Si," 57th Electronic Materials Conference (EMC 2015), The Ohio State University, Columbus, Ohio, Jun. 2015.
24. Z. Mi, S. Zhao, X. Liu, A. T. Connie, K. H. Li, and Q. Wang, "High efficiency AlGaN deep ultraviolet nanowire LEDs and lasers on Si," SPIE Photonics West (SPIE Photonics West 2015), San Francisco, California, United States, Feb. 2015.

Number of Presentations: 24.00

Non Peer-Reviewed Conference Proceeding publications (other than abstracts):

Received Paper

TOTAL:

Number of Non Peer-Reviewed Conference Proceeding publications (other than abstracts):

Peer-Reviewed Conference Proceeding publications (other than abstracts):

Received Paper

TOTAL:

Number of Peer-Reviewed Conference Proceeding publications (other than abstracts):

(d) Manuscripts

Received Paper

TOTAL:

Number of Manuscripts:

Books

Received Book

TOTAL:

Received	Book Chapter

TOTAL:

Patents Submitted

1. Z. Mi, S. Zhao, R. Wang, "High Efficiency Visible and Ultraviolet Nanowire Emitters", US 62/172.874, 2016
2. Z. Mi, H. P. Nguyen, and S. Zhao, "Methods and devices for solid state nanowire devices", US 20,160,027,961, 2016

Patents Awarded

Awards

Zetian Mi was elected Fellow of SPIE.

Graduate Students

NAME	PERCENT_SUPPORTED
FTE Equivalent:	
Total Number:	

Names of Post Doctorates

NAME	PERCENT_SUPPORTED
FTE Equivalent:	
Total Number:	

Names of Faculty Supported

NAME	PERCENT_SUPPORTED
FTE Equivalent:	
Total Number:	

Names of Under Graduate students supported

NAME	PERCENT_SUPPORTED
FTE Equivalent:	
Total Number:	

Student Metrics

This section only applies to graduating undergraduates supported by this agreement in this reporting period

The number of undergraduates funded by this agreement who graduated during this period: 0.00

The number of undergraduates funded by this agreement who graduated during this period with a degree in science, mathematics, engineering, or technology fields:..... 0.00

The number of undergraduates funded by your agreement who graduated during this period and will continue to pursue a graduate or Ph.D. degree in science, mathematics, engineering, or technology fields:..... 0.00

Number of graduating undergraduates who achieved a 3.5 GPA to 4.0 (4.0 max scale):..... 0.00

Number of graduating undergraduates funded by a DoD funded Center of Excellence grant for Education, Research and Engineering:..... 0.00

The number of undergraduates funded by your agreement who graduated during this period and intend to work for the Department of Defense 0.00

The number of undergraduates funded by your agreement who graduated during this period and will receive scholarships or fellowships for further studies in science, mathematics, engineering or technology fields: 0.00

Names of Personnel receiving masters degrees

NAME

Total Number:

Names of personnel receiving PHDs

NAME

Total Number:

Names of other research staff

NAME	PERCENT_SUPPORTED

FTE Equivalent:

Total Number:

Sub Contractors (DD882)

Inventions (DD882)

Scientific Progress

See attachment.

Technology Transfer

Project Report

1. Statement of the Problem Studied

Deep ultraviolet (UV) light sources are essentially required for a broad range of applications including materials processing, bio-chemical detection, water purification, and disinfection. In this regard, significant strides have been made in AlGaN quantum well lasers in the past decade [1-13]. To date, however, the shortest operation wavelength for semiconductor quantum well lasers is limited to ~ 336 nm under electrical injection [14]. Albeit optically pumped DUV lasers have been reported down to ~214 nm [10], the lasing threshold is prohibitively large, on the order of 10^5 to 10^6 W/cm^2 [5]. The poor performance of deep UV optoelectronic devices is largely related to the presence of extremely large densities of threading dislocations (typically in the range of 10^8 cm^{-2}, or higher), strong polarization field and the related quantum-confined Stark effect, and extremely poor p-type conductivity of AlN (hole concentration in AlN typically limited to ~ 10^{11} cm^{-3}, or less) [6, 15-19].

We have recently demonstrated that the afore-described challenges for achieving high performance deep UV lasers can be fundamentally addressed by the emerging AlGaN nanowire structures [20-33]. We have performed a detailed investigation of the molecular beam epitaxial growth and characterization of Al-rich AlGaN nanowire heterostructures. We have discovered that AlGaN quantum dot-like nanostructures can be spontaneously formed in nearly defect-free AlGaN nanowire structures, which can provide superior three-dimensional quantum-confinement of charge carriers and drastically reduce the transparent carrier density compared to conventional quantum wells [27]. Moreover, both Si and Mg dopant incorporation can be significantly enhanced in nanowire structures, due to the much reduced formation energy in nanowires, thereby leading to highly efficient current conduction that was not previously possible [30, 34, 35]. We have further demonstrated, for the first time, electrically pumped AlGaN nanowire lasers operating in the UV-B and UV-C bands [24, 27, 28, 31]. These achievements are summarized below.

2. Summary of the Most Important Results

2.1. Three-dimensional quantum confinement of charge carriers in nearly defect-free AlGaN nanowire arrays

We have systematically investigated the molecular beam epitaxial growth and characterization of AlGaN ternary nanowires, and have demonstrated emission wavelength tunability of AlGaN nanowires in the UV-B and UV-C bands by varying the alloy compositions [22]. Moreover, we have performed detailed structural characterization of AlGaN ternary nanowires grown on Si substrate by scanning transmission electron microscopy (STEM). We have identified that as Al content increases, strong Al and Ga compositional modulation can occur [25, 27]. The top panel of Fig. 1(a) shows the high-angle annular dark-field (HAADF) Z-contrast image of a single AlGaN nanowire, with the bottom panel showing the corresponding RGB pseudo-color image of Ga- and Al-signals. It is clearly seen that there is low Al concentration in the nanowire bulk region and high Al concentration in the near-surface region. The presence of Al-rich AlGaN

shell is attributed to the unique Al migration kinetics under nitrogen rich conditions. Such Al-rich AlGaN shell can suppress the surface nonradiative recombination, thereby leading to significantly enhanced carrier injection efficiency and emission efficiency for AlGaN nanowire LEDs and lasers. Figure 1(b) shows a high-magnification STEM image of an AlGaN nanowire with an average Al content of 10% (estimated by the PL peak position). It is seen that the nanowire bulk region exhibits uniform compositional distribution. However, with further increasing Al composition, strong *atomic scale compositional modulation* can be seen, illustrated in Fig. 1(c). The bright stripes correspond to Ga-rich AlGaN regions. Detailed studies further suggested such Ga-rich AlGaN nanoclusters have dimensions of ~0.25 to 2 nm along the growth direction, and of ~2 to 10 nm along the lateral direction (perpendicular to the growth direction). The localized variations in the Ga-concentration have further been estimated to be 5 – 10 at.%. In addition, both *m*- and *a*-plane orientation views of the Ga-rich AlGaN regions suggest that the Ga-rich regions make up a large portion of the projected thickness within the nanowire diameter (in order to be detectable), which, together with the observed lateral discontinuity, indicates that the atomic-scale fluctuations possess quantum dot/dash-like characteristics, and thus provide three-dimensional quantum-confinement of charge carriers.

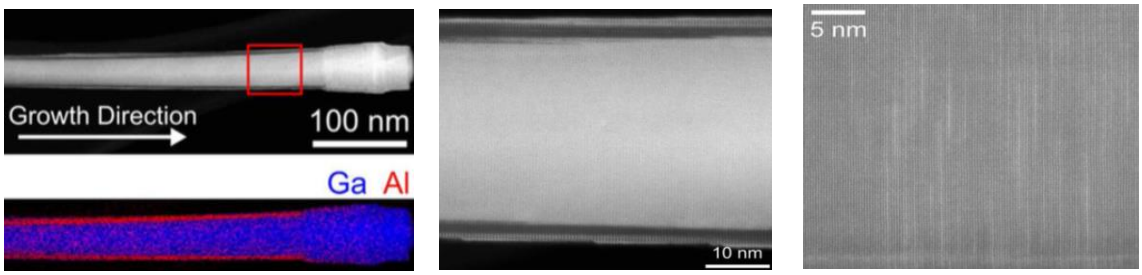

(a) (b) (c)

Figure 1: (a) An HAADF Z-contrast image of a single AlGaN nanowire with the corresponding RGB pseudo-color elemental mapping. (b) and (c) A high-resolution HAADF Z-contrast image of a low Al content nanowire and a high Al content nanowire, respectively.

Illustrated in Fig. 2(a) are the PL spectra measured from a few AlGaN nanowire samples [25, 27]. It is seen that as the Al composition increases, the PL spectral linewidth increases, which is consistent with the inhomogeneous broadening due to the presence of quantum dot-like nanostructures. Also due to the three-dimensional quantum-confinement of charge carriers in nearly defect-free nanowires, an extremely high internal

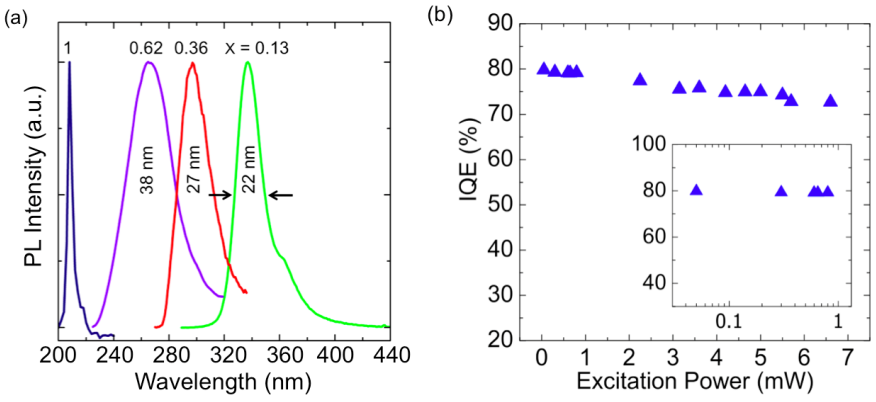

Figure 2: (a) PL spectra of ensemble $Al_xGa_{1-x}N$ nanowires measured at room temperature. The PL spectrum of AlN nanowires is also shown for a comparison. (b) Variations of internal quantum efficiency (IQE) of Al-rich AlGaN nanowires vs. excitation power at room temperature.

quantum efficiency (~70-80%) was measured at room temperature over a wide range of excitation powers, assuming the luminescence emission efficiency is unity at 10 K.

2.2. Impurity band conduction in Al(Ga)N nanowires

We have also systematically investigated the growth and characterization of Mg doped AlN nanowires [20, 25, 32]. To reduce Mg surface desorption, the substrate temperature was reduced compared to the growth temperature of AlN nanowires. Under optimized growth conditions, Mg-doped AlN nanowires exhibited relatively uniform size distribution. Photoluminescence properties have been investigated. Shown in Fig. 3(a) is the PL spectrum of Mg-doped AlN nanowires at room temperature. It is seen that besides the excitonic emission at ~207 nm, another low energy peak can be clearly observed, which is separated from the band edge emission by ~ 0.5 eV. This energy separation is consistent with the Mg activation energy in AlN, suggesting this low energy PL peak is due to Mg acceptor energy level related radiative recombination [17]. In addition, it is noted that the Mg acceptor related transition is highly asymmetric, which partly overlaps with the band edge emission peak (excitonic emission from nondoped AlN nanowires is also shown in Fig. 3(a) for a comparison). At high Mg conceptions, Mg impurity band can be formed. The formation of Mg impurity band can lead to hole conduction through Mg impurity band with much smaller activation energy compared to the energy needed for valence band holes.

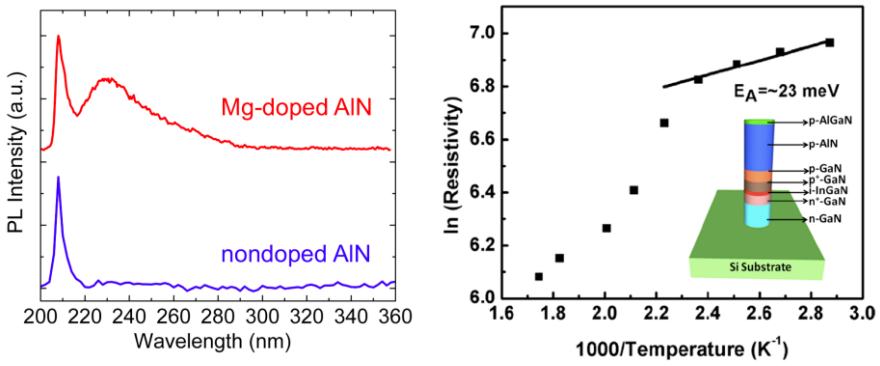

(a) (b)

Figure 3: (a) PL spectrum of Mg-doped AlN nanowires measured at room temperature. PL spectrum of non-doped AlN nanowires is also shown for comparison. (b) Temperature dependent resistivity measured from Mg-doped AlN nanowires, with the inset showing the layer-by-layer structure of the device.

Efficient hole hopping conduction in the Mg impurity band is further confirmed by studying the electrical properties of Mg-doped AlN nanowires [20, 32]. Here the average free hole concentration of Mg-doped AlN nanowires was estimated by large area AlN nanowire devices on Si. The device structure is schematically shown in the inset of Fig. 3(b). In such a structure, the dominant resistance is from Mg-doped AlN segment. Free hole concentration on the order of 10^{16} cm^{-3} was derived at room temperature. Additionally, detailed temperature dependent studies further indicated that the p-type conduction was associated with an activation energy of only ~ 20-30 meV (illustrated in Fig. 3(b)), which is much smaller than the Mg-activation energy in AlN (~0.5 eV) and is consistent with impurity band hoping conduction.

To understand the reason, we have further performed first-principle calculation of Mg dopant formation in AlN nanowires [30]. It was found that the Al-substitutional Mg formation energy was much lower in the near-surface region compared to the bulk region, due to the reduced strain associated with the large surface of nanowires. As a consequence, Mg dopant concentration can be significantly enhanced in AlN nanowires, compared to AlN planar structures. Therefore, the Mg impurity band hole conduction is a natural consequence of high Mg doping concentration due to the enhanced surface doping. Moreover, such AlN nanowires were grown under nitrogen-rich conditions; therefore, the formation of nitrogen vacancy related defects (donors) was greatly minimized.

We have also investigated electrical transport properties of AlN:Mg single nanowire transistors [20]. Figure 4(a) shows the schematic of a Mg-doped AlN single nanowire transistor with a back-gate configuration. An SEM image of a fabricated single nanowire transistor is shown in Fig. 4(b). Back-gate voltage (V_{GD}) dependent source-drain current (I_{SD}) vs. source-drain voltage (V_{SD}) is shown in Fig. 4(c). It is seen that the channel conductance (I_{SD}/V_{SD}) exhibits a clear increase as more negative V_{GD} is applied, suggesting a *p*-type conduction [34, 36]. The transfer characteristics are shown in Fig. 4(d) at V_{SD} = 0.2 V. It is seen that I_{SD} reaches a minimum at V_{GD} ~0.5V, indicating a *p*-type conduction at V_{GD} = 0 V.

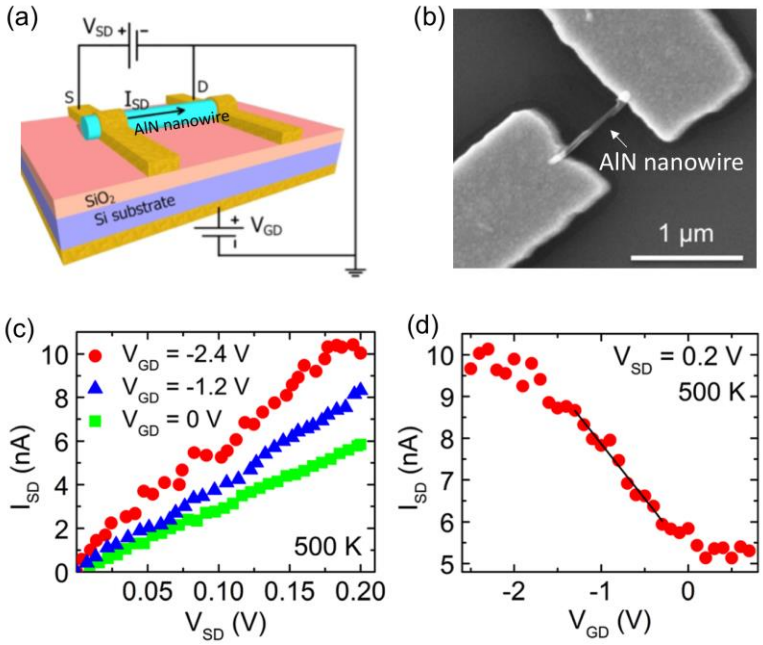

Figure 4: (a) A schematic of Mg-doped AlN nanowire transistor. (b) The corresponding SEM image. (c) I_{SD} vs. V_{SD} under different V_{GD} measured at 500 K from a single Mg-doped AlN nanowire transistor. (d) The corresponding transfer characteristics with V_{SD} = 0.2 V.

Hole mobility values have been further derived [20]. Shown by the blue squares in Fig. 5(a), at room temperature, hole mobility is ~0.67 $cm^2/V{\cdot}s$, corresponding to a free hole concentration of 5.4×10^{15} cm^{-3}, illustrated by blue squares in Fig. 5(b). With the increase of Mg-doping concentration, the hole mobility is reduced, consistent with the enhanced impurity scattering. For the low-doped sample, the hole concentration is ~5.4×10^{15} cm^{-3} at room-temperature and shows a small increase with temperature. The hole concentration increases dramatically with temperature above 600 K, due to the thermal ionization of Mg dopants. Such a temperature-dependent behavior is consistent with impurity band conduction and valence band conduction at low and high temperatures, respectively. The significant effect of impurity band conduction is

more evident in the high-doped sample. The hole concentration reaches as high as 6×10^{17} cm^{-3} at room-temperature, which is nearly seven orders of magnitude higher than previously reported values (~10^{10} cm^{-3}) for Mg-doped AlN epilayers. Moreover, the hole concentration exhibits a *decreasing* trend with increasing temperature in the range of 300 K to 550 K, followed by an increase with temperature from 550 K to 650 K. Such an anomalous temperature-dependent hole concentration can be well explained by the two-band conduction model. The hole concentrations in the impurity and valence bands exhibit different temperature-dependent behaviors: The effective hole concentration in the impurity band decreases with temperature, whereas hole concentration in the valence band increases with temperature. Consequently, the dominance of impurity band conduction near room-temperature leads to a decrease of hole concentration from 300 K to 550 K. With further increasing temperature, the contribution from holes in the valence band becomes more important, and the overall hole concentration shows an increasing trend with temperature. Such a unique temperature-dependent hole concentration has been previously measured in GaN in a lower temperature range [20].

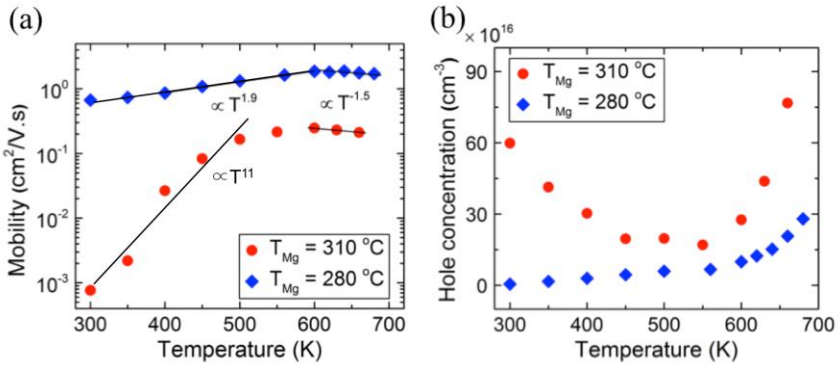

Figure 5: (a) and (b) Hole mobility and concentration vs. temperature for AlN:Mg nanowires with low and high doping concentrations.

Factors that contribute to such unusually efficient p-type conduction in ultra-wide-bandgap Al(Ga)N are described as follows. i) Al(Ga)N nanostructures exhibit drastically reduced defect densities, compared to Al(Ga)N epilayers. Moreover, the use of plasma-assisted MBE can significantly reduce impurity incorporation, such as carbon, compared to AlGaN grown by CVD or MOCVD. ii) The use of nitrogen-rich epitaxy conditions suppress the formation of nitrogen-vacancy related defects (donors) in Al(Ga)N. iii) Recent first-principles calculations have revealed that the Al-substitutional Mg formation energy is drastically reduced in AlGaN nanowire structures, compared to that in AlGaN epilayers, thereby leading to significantly enhanced Mg-dopant incorporation and the formation of Mg impurity band in Al(Ga)N nanostructures. iv) Another critical advantage associated with the enhanced Mg-dopant incorporation is that a portion of the Mg-dopants have significantly reduced ionization energy, due to the band tailing effect and the significantly broadened Mg energy levels, which is evidenced by the partial overlap between the excitonic emission and the Mg acceptor related radiative recombination transition peaks shown in Fig. 3(a).

2.3. Surface emitting AlN nanowire LEDs

We have also demonstrated the first AlN nanowire LEDs [29, 30]. The device structure is shown in Fig. 6(a), which consists of n-GaN, p-i-n AlN, and p-AlGaN contact layer. A direct metal deposition at a tilting angle, consisting of 15 nm Ni/10 nm Au was employed to form p-contact

on the nanowire top surface. In the device fabrication process, no polymer passivation was used, in order to avoid any deep UV light absorption. A schematic of the fabricated device is also shown in Fig. 6(a). A top-view SEM image after the top p-metal deposition is shown in Fig. 6(b). It is seen that such metal contact can connect the nanowire tops very well. Figure 6(c) shows the I-V characteristics of AlN nanowire LEDs measured at different temperatures. The device exhibits excellent current-voltage characteristics. The turn-on voltage is ~ 5.5 V, which is consistent with the bandgap energy of AlN. Moreover, at 20 A/cm^2, the forward voltage is only 7 V, which corresponds to an electrical efficiency ~ 85 % considering the photon energy of ~ 6 eV. This electrical performance is drastically improved compared to previously reported planar AlN LEDs [17], which can be largely ascribed to the significantly enhanced Mg-dopant incorporation in nanowire structures and the resulting efficient impurity band hole conduction. The impurity band hole conduction is further supported by the nearly temperature-independent resistance shown in Fig. 6(c).

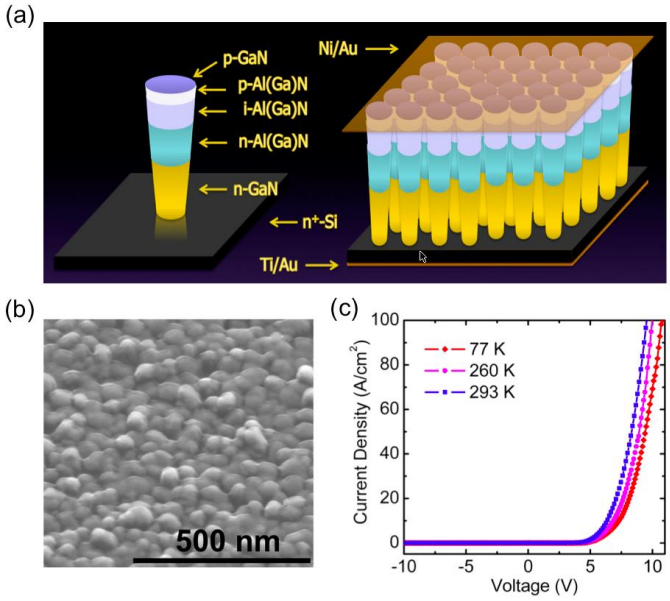

Figure 6: (a) Schematic of AlN nanowire LEDs (Left: the structure; Right: the fabricated device). (b) An SEM image of the device top surface after p-metal deposition. (c) I-V curves of AlN nanowire LEDs measured under different temperatures.

Electroluminescence (EL) characteristics at room temperature have been further investigated. The measurement setup is schematically shown Fig. 7(a). The EL spectra were collected by an optical fiber. By changing the fibre position EL emission from different angles can be measured. The 90 degree detection angle (with respective to the x-axis) means the fiber is positioned directly on the top surface of the device. The EL spectra measured directly from the top surface under a pulsed bias are shown in Fig. 7(b). A strong emission peak around 207 nm is measured. There is no shift of the emission wavelength with increasing current, suggesting a robust exciton emission. The integrated EL intensity is shown in Fig. 7(c). It is seen that the intensity increases nearly linearly with injection current. The angle dependent EL emission was also measured. Illustrated in Fig. 7(d), as the detection angle reduces, the EL intensity also decreases, indicating the light is emitted primarily from the top surface. Light emission in AlN is intrinsically TM polarized, with the electric field parallel along the nanowire c-axis (E||c), which generally prevents light extraction from the top surface. In AlN nanowire LEDs, however, the light extraction from the nanowire top surface, i.e., along the c-axis, can be made possible by optimizing the nanowire size and spacing, due to the multiple light coupling and scattering process amongst nanowires [29].

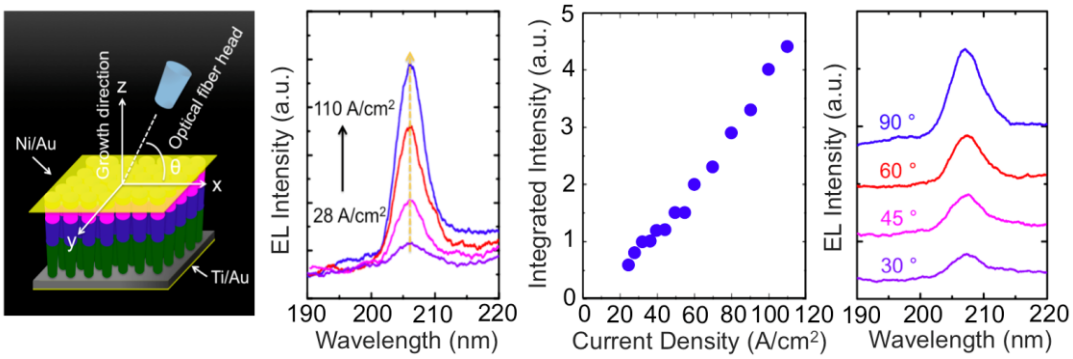

(a) (b) (c) (d)

Figure 7: (a) The schematic of the EL measurement configuration. (b) The EL spectra measured under different current density from the device top surface (pulsed). (c) The integrated EL intensity vs. current density from (b). (d) The angle dependent EL intensity.

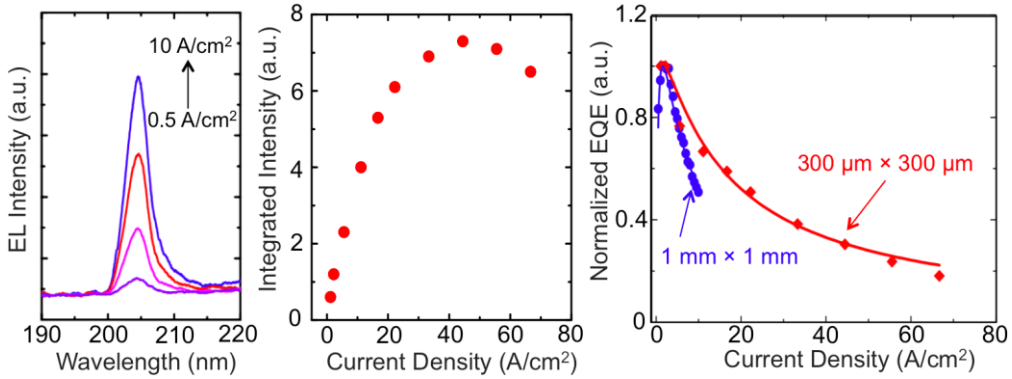

(a) (b) (c)

Figure 8: (a) The EL spectra of AlN nanowire LEDs measured under different injection currents at low temperature. (b) The integrated EL intensity vs. the current density. (c) The normalized relative EQE vs. the current density for two different devices. The solid lines are fitting curves by the ABC model.

The low temperature EL emission characteristics have also been studied (at 77 K). Illustrated in Fig. 8(a) is the EL spectra measured from the device top surface under different injection currents. It is seen that strong EL peak, centered around 204 nm, is measured. Compared to the room temperature EL spectra, the peak wavelength is blue-shifted, due to the increased bandgap energy. In addition, it is noted that the EL peak was also measured below the bandgap voltage (~ 6 V), suggesting extremely efficient current injection into the device active region. The integrated EL intensity vs. the injection current density is shown in Fig. 8(b). It is seen that as the injection current increases, the light output first increases rapidly, followed by a saturation, and then a drop. The derived relative external quantum efficiency (EQE, defined by the light output power divided by the current density) is shown in Fig. 8(c). It is seen that the EQE exhibits a sharp increase as the injection current increases, followed by a rapid decrease, which is mainly attributed to the lack of carrier confinement in the active region and the resulting large electron overflow. This EQE trend can be well simulated by the ABC model. *A*, *B*, and *C* parameters in the range of 5×10^{6} s^{-1}, 4×10^{-9} $cm^{3}s^{-1}$, and 6×10^{-26} $cm^{6}s^{-1}$, respectively, were derived. Compared

to InGaN/GaN nanowire LEDs (wherein A is in the range of 10^{7-8} s^{-1}, the A value here is much smaller. This is due to the smaller surface recombination velocity of AlN compared to InGaN. The C value, however, is much larger, which is mainly attributed to the electron overflow in the presented AlN LEDs with a homojunction structure [29].

2.4. Electrically injected AlGaN nanowire lasers operating in the UV-B band

Compared to lasers based on conventional GaN/AlGaN multiple quantum wells, AlGaN nanowire lasers are much less explored [4, 14, 37-39]. Recently, by exploiting Anderson localization of light in nearly defect-free AlGaN nanowires grown by MBE, we have demonstrated electrically injected lasers in the UV-AII band at 6 K [31]. The threshold current density is in the range of tens of A/cm^2, which is nearly two to three orders of magnitude lower compared to the previously reported GaN/AlGaN multiple quantum well lasers in the similar wavelength range [14]. Moreover, by further increasing Al content, we have demonstrated electrically injected lasers with AlGaN ternary nanowire in the UV-B and UV-C bands [24, 27, 28].

The electrically injected lasers in the UV-B band are first described [27]. The AlGaN nanowire laser heterostructures is schematically shown in Fig. 9(a), which consists of GaN:Si (~ 250 nm), AlGaN:Si (~ 100 nm), AlGaN (~ 100 nm), AlGaN:Mg (~ 100 nm), and GaN:Mg (~ 10 nm) layers. Such vertically aligned, randomly distributed AlGaN nanowire arrays can lead to strong photon confinement, due to the Anderson localization of light. The degree of such photon confinement depends on the nanowire size, spacing, and filling factor. By optimizing these factors, high Q optical cavities (λ ~ 290 nm) can be obtained in spontaneously formed AlGaN nanowire arrays. Figure 9(b) shows the corresponding electrical field distribution in such AlGaN nanowire arrays. It is seen that strong light confinement can be achieved, due to such recurrent, multiple scattering process. Another important factor needs to be considered is the optical confinement along the nanowire vertical direction, which can be made possible by the inversely tapered nanowire morphology, i.e., increasing nanowire diameter along the growth direction. Illustrated in Fig. 9(c), the effective refractive index reaches minimum at nanowire/Si interface, due to such inversely tapered morphology, thereby greatly minimizing optical loss through the underlying GaN nanowire template and Si substrate. The optical field profile along the nanowire vertical direction is also shown in Fig. 9(c). In this calculation, the p-metal layer was also considered. It is seen that strong optical confinement in the AlGaN active region is clearly achieved.

The subsequent device fabrication process involves the use of standard photolithography and contact metallization techniques. The temperature dependent EL spectra are shown in Fig. 9(d). The emitted light is collected from the nanowire top with a deep UV objective, and detected by a charge-coupled device (CCD) that is attached to a high-resolution spectrometer. It is seen that at 10 μA (the bottom curve), only a very broad spontaneous emission spectrum is measured. As the injection current increases, a sharp peak around 289 nm appears (the top curve is at 10 μA). The integrated EL intensity vs. the injection current is shown in Fig. 9(e). A clear light amplification is seen, with a clear threshold around 30 μA. As a comparison, the background emission is also investigated. The black triangles in Fig. 9(e) represent the integrated EL intensity of the boxed region from Fig. 9(d). It is seen that the background emission remains nearly constant, due to the

clamping of carrier concentration above threshold. In addition, it is noted that a very small increase of the background emission exists with further increasing current, which is commonly measured from quantum dot lasers, mainly due to the inhomogeneous broadening and hot carrier effect [40]. The inset of Fig. 9(e) shows the spectral linewidth vs. the injection current. A significant reduction in the spectral linewidth is measured at threshold.

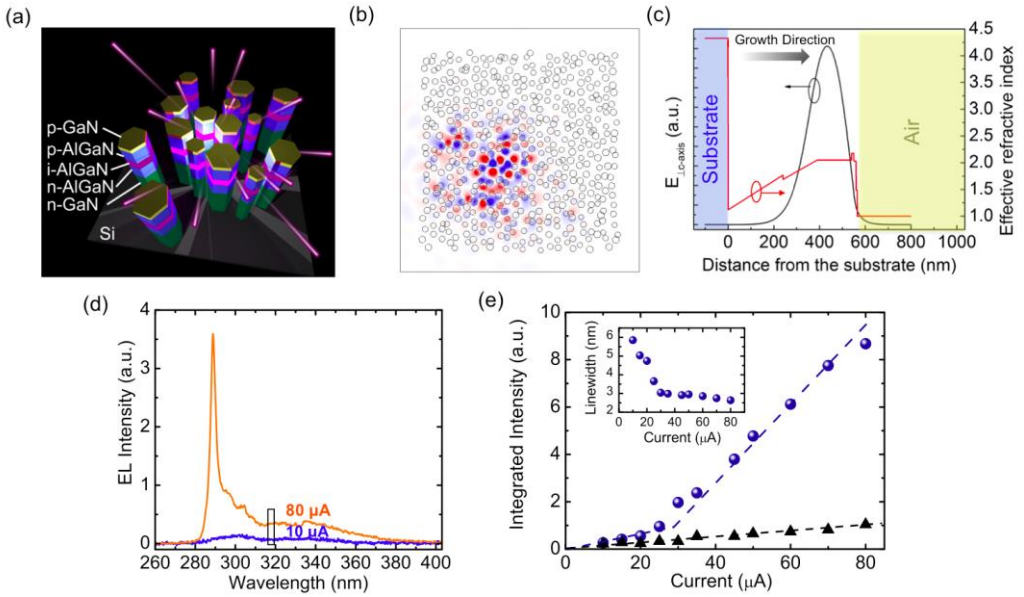

Figure 9: (a) The schematic of the AlGaN nanowire random laser on Si substrate, with each layer labeled. (b) The simulated optical field distribution at a wavelength of 290 nm for a random nanowire array cavity. (c) The electric field (left axis) and effective refractive index (right axis) as a function of the distance from substrate. (d) The EL emission spectra measured under continuous-wave operation at 10 μA and 80 μA at room temperature. (e) The integrated EL intensity vs. the injection current. Blue circles represent the lasing peak. Black triangles denote the background emission from the box area in Fig. (d) with a linewidth of 2 nm. The inset shows the EL spectral linewidth vs. the injection current. Dashed lines are guide-for-eye.

The device lasing area is around 10 μm^2. This gives a threshold current density around 300 A/cm^2, which is significantly smaller compared to AlGaN quantum well lasers operating at 336 nm [14]. This low lasing threshold is largely attributed to the discrete density of states associated with the quantum dot-like nanostructures, the nearly defect-free AlGaN nanowires, and the high Q-factor of Anderson localization in self-organized nanowire arrays.

2.5. Electrically injected AlGaN nanowire lasers operating in the UV-C band

By further changing alloy composition, such electrically injected AlGaN nanowire lasers can also be realized in the UV-C band [28]. Illustrated in Fig. 10(a) are the EL spectra measured at 77 K under a continuous-wave biasing. It is seen that as the injection current increases, a sharp peak centered around 262 nm appears. Shown in Fig. 10(b) are the integrated EL intensity of the background emission (in black squares, from the boxed region in Fig. 10(a)) and the main peak (in blue circles). It is seen that as the injection current increases, the intensity of the background emission only increases slightly. In contrast, the intensity of the main peak exhibits a sharp

rising, indicating a light amplification. The inset of Fig. 10(b) shows the integrated EL intensity of the main peak in a logarithmic scale, and a clear s-shape, corresponding to linear spontaneous emission, super-linear amplified spontaneous emission, and linear lasing emission, can be observed. This provided unambiguous evidence that the main peak is a lasing peak. The threshold current density is only 200 A/cm^2, which is larger compared to the previously discussed AlGaN nanowire lasers in the UV-A band, but is significantly smaller compared to AlGaN quantum well lasers at 336 nm. Figure. 10(c) shows the linewidth reduction from 1.2 nm to 0.3 nm near the threshold. Figure 10(d) shows that the lasing peak remains highly stable above the threshold with no obvious wavelength shift.

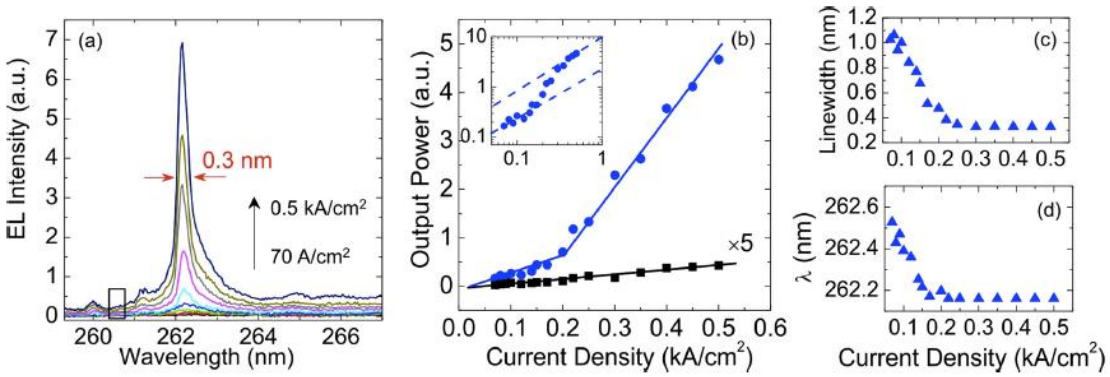

Figure 10: (a) The EL spectra of an AlGaN nanowire laser operating at 262 nm. The measurement is performed at 77 K under a continuous wavelength operation. (b) The integrated EL intensity vs. the injection current. Blue circles represent the lasing peak. Black squares denote the background emission from the box area in (a) with a linewidth of 0.3 nm. The inset shows the plot in a logarithmic scale. (c) and (d) Linewidth and peak wavelength vs. current density, respectively.

Room-temperature electrically injected AlGaN nanowire lasers operating at 239 nm have been further demonstrated [24]. The emission spectra of a 239 nm AlGaN nanowire laser device measured at room temperature are shown in Fig. 11(a). The light emission is collected by a deep UV objective from the device top surface, spectrally resolved by a high-resolution spectrometer and detected by a CCD camera. It is seen that under a low injection current, only a very broad emission spectrum is measured. With the increase of injection current, a sharp peak centered at 239 nm appears. The light intensity vs. injection current is shown in Fig. 11(b), which exhibits a distinct lasing threshold at 0.35 mA. Figure 11 (c) shows the linewidth reduction from 1.7 nm to 0.9 nm near the threshold. A non-lasing cavity mode (~267 nm) is also analyzed. As can be seen in Fig. 11(b), its intensity stays nearly constant above the threshold, further supporting the lasing at 239 nm.

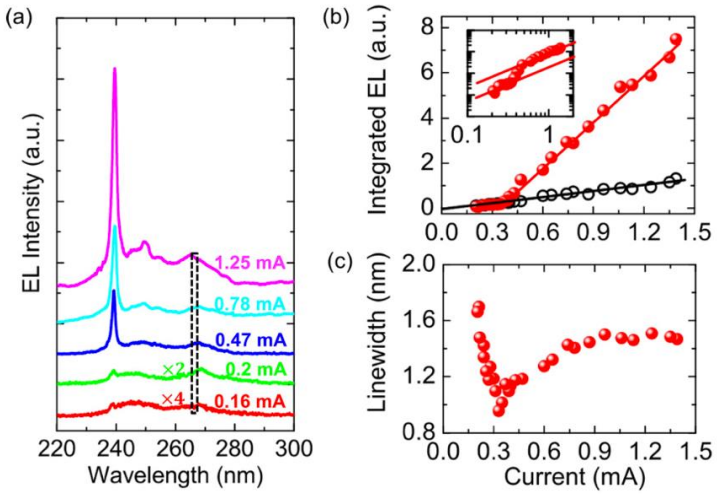

Figure 11: (a) The emission spectra measured under continuous-wave biasing for an AlGaN nanowire laser at 239 nm. (b) The integrated intensity as a function of injection current. Red filled circles: the lasing peak. Black open triangles: non-lasing cavity mode from the boxed region in (a). The inset shows the L-I curve of the lasing peak in a logarithmic scale. (c) The linewidth reduction of the lasing peak.

3. Publications

Journal Papers:

1. N. H. Tran, B. H. Le, S. Zhao, and Z. Mi, "On the mechanism of highly efficient p-type conduction of Mg-doped ultra-wide-bandgap AlN nanostructures", Appl. Phys. Lett., vol. 110, 032102, 2017.
2. S. M. Sadaf, S. Zhao, Y. Wu, Y.-H. Ra, X. Liu, S. Vanka, and Z Mi, "An AlGaN core-shell tunnel junction nanowire light-emitting diode operating in the ultraviolet-C band", Nano Lett., accepted. (10.1021/acs.nanolett.6b05002)
3. S. Zhao, S.M. Sadaf, S. Vanka, Y. Wang, R. Rashid, Z Mi, "Sub-milliwatt AlGaN nanowire tunnel junction deep ultraviolet light emitting diodes on silicon operating at 242 nm", Appl. Phys. Lett., vol. 109, 201106, 2016.
4. S. Zhao, X. Liu, Y. Wu, and Z. Mi, "An electrically pumped 239 nm AlGaN nanowire laser operating at room temperature", Appl. Phys. Lett., vol. 109, 191106 (2016).
5. B. Le, S. Zhao, X. Liu, S. Y. Woo, G. A. Botton, and Z. Mi, "Controlled coalescence of AlGaN nanowire arrays: An architecture for dislocation-free planar ultraviolet photonic device applications", Adv. Mater., vol. 28, 8446-8454, 2016.
6. S. Zhao, S. Woo, M. Bugnet, X. Liu, J. J. Kang, G. Botton, and Z. Mi, "Three-dimensional quantum confinement of charge carriers in self-organized AlGaN nanowires: A viable route to electrically injected deep ultraviolet lasers", Nano Lett. 15, 7801 (2015).
7. S. Zhao, M. Djavid, and Z. Mi, "Surface emitting, high efficiency near-vacuum ultraviolet light source with aluminum nitride nanowires monolithically grown on Si", Nano Lett. 15, 7006 (2015).
8. S. Zhao, X. Liu, S. Woo, J. J. Kang, G. Botton, and Z. Mi, "An electrically injected AlGaN nanowire laser operating in the UV-C band", Appl. Phys. Lett. 107, 043101 (2015).
9. S. Zhao, A. T. Connie, M. H. T. Dastjerdi, X. H. Kong, Q. Wang, M. Djavid, S. Sadaf, X. D. Liu, I. Shih, H. Guo, and Z. Mi, "Aluminum nitride nanowire light emitting diodes: Breaking the fundamental bottleneck of deep ultraviolet light sources", Sci. Rep. 5, 8332 (2015).
10. K. H. Li, X. Liu, Q. Wang, S. Zhao, and Z. Mi, "Ultralow threshold, electrically injected

AlGaN nanowire ultraviolet lasers on Si", Nature Nanotechnol. 10, 140 (2015).

11. A. T. Connie, S. Zhao, S. Sadaf, I. Shih, Z. Mi, X. Du, J. Y. Lin, and H. X. Jiang, "Optical and electrical properties of Mg-doped AlN nanowires grown by molecular beam epitaxy", Appl. Phys. Lett. 106, 213105 (2015).

Conferences:

1. **(Invited)** S. Zhao, X. Liu, and Z. Mi, "Electrically injected AlGaN nanowire deep ultraviolet lasers on Si," SPIE Photonics West, San Francisco, CA, Jan. 30-Feb. 2, 2017.
2. **(Invited)** Z. Mi, S. Zhao, and S. Sadaf, "AlGaN nanowire light emitting diodes: Breaking the efficiency bottleneck of deep ultraviolet light sources," SPIE Photonics West, San Francisco, CA, Jan. 30-Feb. 2, 2017.
3. **(Keynote)** Z. Mi, "Emerging applications of III-nitride nanostructures: From deep UV photonics to artificial photosynthesis," UK Nitrides Consortium Conference, Oxford, UK, Jan. 5-6, 2017.
4. S. M. Sadaf, S. Zhao, Y. Wu, Y.-H. Ra, X. Liu, and Z. Mi, "Tunnel junction enhanced high power deep ultraviolet nanowire light emitting diodes," 32nd North American Molecular Beam Epitaxy Conference, Saratoga Springs, NY, Sept. 18-21, 2016.
5. S. Zhao, S. Sadaf, X. Liu, and Z. Mi, "Molecular beam epitaxial growth and characterization of AlGaN nanowires for 240 nm emitting UV LEDs and lasers," 32nd North American Molecular Beam Epitaxy Conference, Saratoga Springs, NY, Sept. 18-21, 2016.
6. **(Invited)** Z. Mi, S. Zhao, X. Liu, S. Y. Woo, M. Bugnet, and G. A. Botton, "Electrically injected AlGaN nanowire deep ultraviolet lasers," IEEE Photonics Conference, Waikoloa, Hawaii, Sept. 2-6, 2016.
7. S. Zhao, X. Liu, S. Y. Woo, Y. Wu, S. Sadaf, R. Rashid, Y. Wang, D. Laleyan, G. A. Botton, and Z. Mi, "AlGaN nanowire deep UV LEDs and lasers operating below 240 nm," International Workshop on Nitride Semiconductors, Orlando, FL, Oct. 2-7, 2016.
8. **(Invited)** Z. Mi, S. Zhao, X. Liu, S. Y. Woo, M. Bugnet, and G. A. Botton, "Al(Ga)N nanowire deep ultraviolet light emitting diodes and lasers," International Conference on Molecular Beam Epitaxy (ICMBE 2016), Montpellier, France, Sept. 4-9, 2016.
9. **(Invited)** Z. Mi and S. Zhao, "AlGaN nanowire deep ultraviolet LEDs and lasers," 2016 IEEE Summer Topical Meeting on Nanowire Optoelectronics, Newport Beach, CA, July 11-13, 2016.
10. **(Invited)** Z. Mi and S. Zhao, "Electrically Pumped Lasers and Light Emitting Diodes in the Ultraviolet-C Band with AlGaN Nanowires," 229th ECS Meeting, San Diego, CA, May 29 - June 3, 2016.
11. **(Invited)** Z. Mi, S. Zhao, X. Liu, S. Y. Woo, and G. A. Botton, "Electrically injected AlGaN nanowire deep ultraviolet lasers on Si", SPIE Photonics West (SPIE Photonics West 2016), San Francisco, California, United States, Feb. 2016.
12. S. Zhao, D. Laleyan, M. Djavid, B. H. Le, X. Liu, and Z. Mi, "A surface-emitting electrically-injected near vacuum ultraviolet light source with aluminum nitride nanowires", SPIE Photonics West (SPIE Photonics West 2016), San Francisco, California, United States, Feb. 2016.
13. **(Keynote)** Z. Mi, S. Zhao, X. Liu, B. H. Le, M. G. Kibria, F. A. Chowdhury, "Tuning the surface charge properties of III-nitride nanowires: From ultralow threshold deep UV lasers to high efficiency artificial photosynthesis", The 6th International Symposium on Growth of III-

Nitrides (ISGN 2015), Hamamatsu, Japan, Nov. 2015.

14. N. H. Tran, S. Zhao, B. H. Le, and Z. Mi, "Impurity-band conduction in Mg-doped AlN nanowires", The 31th North American Molecular Beam Epitaxy Conference (NAMBE 2015), Mayan Riviera, Mexico, Oct. 2015.
15. B. H. Le, S. Zhao, X. Liu, Y. H. Ra, M. Djavid, and Z. Mi, "Electrically injected GaN/AlGaN nanowire ultraviolet lasers by selective area growth", The 31th North American Molecular Beam Epitaxy Conference (NAMBE 2015), Mayan Riviera, Mexico, Oct. 2015.
16. **(Invited)** Z. Mi, S. Zhao, X. Liu, K. H. Li, J. Kang, Q. Wang, S. Y. Woo, and G. Botton "Electrically injected AlGaN nanowire deep UV lasers on Si", 11th International Conference on Nitride Semiconductors (ICNS 2015), Beijing, China, Aug. 2015.
17. S. Zhao, A. T. Connie, M. H. T. Dastjerdi, S. Sadaf, I. Shih, and Z. Mi, "Molecular beam epitaxial growth and characterization of AlN nanowire LEDs on Si", 11th International Conference on Nitride Semiconductors (ICNS 2015), Beijing, China, Aug. 2015.
18. S. Zhao, X. Liu, K.-H. Li, S. Y. Woo, G. Botton, and Z. Mi, "AlGaN nanowire ultraviolet lasers on Si", 2015 IEEE Summer Topicals Meeting Series (SUM-IEEE 2015), Nassau, Bahamas, Jul. 2015.
19. S. Zhao, A. T. Connie, B. H. Le, X. H. Kong, H. Guo, X. Z. Du, J. Y. Lin, H. X. Jiang, I. Shih, and Z. Mi, "p-Type AlN nanowires and AlN nanowire light emitting diodes on Si", 2015 IEEE Summer Topicals Meeting Series (SUM-IEEE 2015), Nassau, Bahamas, Jul. 2015.
20. S. Zhao, A. T. Connie, B. H. Le, I. Shih, and Z. Mi, "Molecular beam epitaxial growth and characterization of AlN nanowire LEDs: Breaking the bottleneck of deep UV light sources," 2015 Compound Semiconductor Week (CSW 2015), University of California, Santa Barbara, California, United States, Jul. 2015.
21. S. Zhao, X. Liu, B. H. Le, J. J. Kang, K. H. Li, Q. Wang, and Z. Mi, "Electrically injected deep ultraviolet lasers based on AlGaN nanostructures," 2015 Compound Semiconductor Week (CSW 2015), University of California, Santa Barbara, California, United States, Jul. 2015.
22. S. Zhao, X. Liu, J. J. Kang, K. H. Li, Q. Wang, and Z. Mi, "Electrically injected AlGaN nanowire ultraviolet lasers," 57th Electronic Materials Conference (EMC 2015), The Ohio State University, Columbus, Ohio, Jun. 2015.
23. S. Zhao, A. T. Connie, M. H. T. Dasterjdi, S. Sadaf, I. Shih, and Z. Mi, "Molecular beam epitaxial growth and characterization of AlN nanowire LEDs on Si," 57th Electronic Materials Conference (EMC 2015), The Ohio State University, Columbus, Ohio, Jun. 2015.
24. Z. Mi, S. Zhao, X. Liu, A. T. Connie, K. H. Li, and Q. Wang, "High efficiency AlGaN deep ultraviolet nanowire LEDs and lasers on Si," SPIE Photonics West (SPIE Photonics West 2015), San Francisco, California, United States, Feb. 2015.

4. Report of Inventions

1. Z. Mi, S. Zhao, R. Wang, "High Efficiency Visible and Ultraviolet Nanowire Emitters", US 62/172.874, 2016
2. Z. Mi, H. P. Nguyen, and S. Zhao, "Methods and devices for solid state nanowire devices", US 20,160,027,961, 2016

5. List of Scientific Personnel Supported, Degrees, Awards and Honors

Songrui Zhao (Postdoctoral researcher), Mehrdad Djavid (PhD student), and Nhung Tran

Mehrdad Djavid received the PhD degree in Aug. 2016.

Nhung Tran received the Outstanding Student Paper Award from the North American Molecular Beam Epitaxy Conference in 2015.

Zetian Mi was elected Fellow of SPIE.

6. Technology Transition

None.

Bibliography:

[1] J. Winder and R. Bibb, "Medical Rapid Prototyping Technologies: State of the Art and Current Limitations for Application in Oral and Maxillofacial Surgery," *Journal of Oral and Maxillofacial Surgery,* vol. 63, pp. 1006-1015, 2005.

[2] J.-L. Boulnios, "Photophysical Processes in Recent Medical Laser Developments: a Review," *Lasers in Medical Science,* vol. 1, p. 47, 1986.

[3] T. Takano, Y. Narita, A. Horiuchi, and H. Kawanishi, "Room-temperature deep-ultraviolet lasing at 241.5 nm of AlGaN multiple-quantum-well laser," *Applied Physics Letters,* vol. 84, p. 3567, 2004.

[4] H. Yoshida, M. Kuwabara, Y. Yamashita, K. Uchiyama, and H. Kan, "The current status of ultraviolet laser diodes," *physica status solidi (a),* vol. 208, pp. 1586-1589, 2011.

[5] V. N. Jmerik, E. V. Lutsenko, and S. V. Ivanov, "Plasma-assisted molecular beam epitaxy of AlGaN heterostructures for deep-ultraviolet optically pumped lasers," *physica status solidi (a),* vol. 210, pp. 439-450, 2013.

[6] M. Martens, F. Mehnke, C. Kuhn, C. Reich, V. Kueller, A. Knauer, *et al.*, "Performance Characteristics of UV-C AlGaN-Based Lasers Grown on Sapphire and Bulk AlN Substrates," *IEEE Photonics Technology Letters,* vol. 26, p. 342, 2014.

[7] H. Sun, J. Woodward, J. Yin, A. Moldawer, E. F. Pecora, A. Y. Nikiforov, *et al.*, "Development of AlGaN-based graded-index-separate-confinement-heterostructure deep UV emitters by molecular beam epitaxy," *Journal of Vacuum Science & Technology B: Microelectronics and Nanometer Structures,* vol. 31, p. 03C117, 2013.

[8] T.-T. Kao, Y.-S. Liu, M. Mahbub Satter, X.-H. Li, Z. Lochner, P. Douglas Yoder, *et al.*, "Sub-250 nm low-threshold deep-ultraviolet AlGaN-based heterostructure laser employing HfO2/SiO2 dielectric mirrors," *Applied Physics Letters,* vol. 103, p. 211103, 2013.

[9] H. Zhu, C.-X. Shan, B.-H. Li, Z. Z. Zhang, D.-Z. Shen, and K.-L. Choy, "Low-threshold electrically pumped ultraviolet laser diode," *Journal of Materials Chemistry,* vol. 21, p. 2848, 2011.

[10] M. G. M. Shatalov, V. Adivarahan, and A. Khan, , "Room-Temperature Stimulated Emission from AlN at 214 nm," *Japanese Journal of Applied Physics,* vol. 45, p. L1286, 2006.

[11] T. K. Sharma and E. Towe, "Why are nitride lasers limited to the spectral range from ~340 to 530 nm?," *physica status solidi (c),* vol. 8, pp. 2366-2368, 2011.

[12] M. S. Shur and R. Gaska, "Deep-Ultraviolet Light-Emitting Diodes," *IEEE Transcations on Electron Devices,* vol. 57, p. 12, 2010.

[13] A. Khan, K. Balakrishnan, and T. Katona, "Ultraviolet light-emitting diodes based on group three nitrides," *Nature Photonics,* vol. 2, p. 77, 2008.

[14] H. Yoshida, Y. Yamashita, M. Kuwabara, and H. Kan, "Demonstration of an ultraviolet 336 nm AlGaN multiple-quantum-well laser diode," *Applied Physics Letters,* vol. 93, p. 241106, 2008.

[15] H. Hirayama, S. Fujikawa, N. Noguchi, J. Norimatsu, T. Takano, K. Tsubaki, *et al.*, "222-282 nm AlGaN and InAlGaN-based deep-UV LEDs fabricated on high-quality AlN on sapphire," *physica status solidi (a),* vol. 206, pp. 1176-1182, 2009.

[16] Y. Taniyasu, M. Kasu, and T. Makimoto, "Increased electron mobility in n-type Si-doped AlN by reducing dislocation density," *Applied Physics Letters*, vol. 89, p. 182112, 2006.
[17] Y. Taniyasu, M. Kasu, and T. Makimoto, "An aluminium nitride light-emitting diode with a wavelength of 210 nanometres," *Nature*, vol. 441, pp. 325-8, 2006.
[18] J. Renard, R. Songmuang, G. Tourbot, C. Bougerol, B. Daudin, and B. Gayral, "Evidence for quantum-confined Stark effect in GaN/AlN quantum dots in nanowires," *Physical Review B*, vol. 80, p. R121305, 2009.
[19] S. F. Chichibu, A. Uedono, T. Onuma, B. A. Haskell, A. Chakraborty, T. Koyama, *et al.*, "Origin of defect-insensitive emission probability in In-containing (Al,In,Ga)N alloy semiconductors," *Nature Materials*, vol. 5, pp. 810-6, 2006.
[20] N. H. Tran, B. H. Le, S. Zhao, and Z. Mi, "On the mechanism of highly efficient p-type conduction of Mg-doped ultra-wide-bandgap AlN nanostructures," *Applied Physics Letters*, vol. 110, p. 032102, 2017.
[21] S. M. Sadaf, S. Zhao, Y. Wu, Y. H. Ra, X. Liu, S. Vanka, *et al.*, "An AlGaN Core-Shell Tunnel Junction Nanowire Light-Emitting Diode Operating in the Ultraviolet-C Band," *Nano Letters*, vol. 17, pp. 1212-1218, 2017.
[22] S. Zhao, S. Y. Woo, S. M. Sadaf, Y. Wu, A. Pofelski, D. A. Laleyan, *et al.*, "Molecular beam epitaxy growth of Al-rich AlGaN nanowires for deep ultraviolet optoelectronics," *APL Materials*, vol. 4, p. 086115, 2016.
[23] S. Zhao, S. M. Sadaf, S. Vanka, Y. Wang, R. Rashid, and Z. Mi, "Sub-milliwatt AlGaN nanowire tunnel junction deep ultraviolet light emitting diodes on silicon operating at 242 nm," *Applied Physics Letters*, vol. 109, p. 201106, 2016.
[24] S. Zhao, X. Liu, Y. Wu, and Z. Mi, "An electrically pumped 239 nm AlGaN nanowire laser operating at room temperature," *Applied Physics Letters*, vol. 109, p. 191106, 2016.
[25] Z. Mi, S. Zhao, S. Y. Woo, M. Bugnet, M. Djavid, X. Liu, *et al.*, "Molecular beam epitaxial growth and characterization of Al(Ga)N nanowire deep ultraviolet light emitting diodes and lasers," *Journal of Physics D: Applied Physics*, vol. 49, p. 364006, 2016.
[26] B. H. Le, S. Zhao, X. Liu, S. Y. Woo, G. A. Botton, and Z. Mi, "Controlled Coalescence of AlGaN Nanowire Arrays: An Architecture for Nearly Dislocation-Free Planar Ultraviolet Photonic Device Applications," *Advanced Materials*, vol. 28, p. 8446, 2016.
[27] S. Zhao, S. Y. Woo, M. Bugnet, X. Liu, J. Kang, G. A. Botton, *et al.*, "Three-Dimensional Quantum Confinement of Charge Carriers in Self-Organized AlGaN Nanowires: A Viable Route to Electrically Injected Deep Ultraviolet Lasers," *Nano Letters*, vol. 15, pp. 7801-7, 2015.
[28] S. Zhao, X. Liu, S. Y. Woo, J. Kang, G. A. Botton, and Z. Mi, "An electrically injected AlGaN nanowire laser operating in the ultraviolet-C band," *Applied Physics Letters*, vol. 107, p. 043101, 2015.
[29] S. Zhao, M. Djavid, and Z. Mi, "A surface emitting, high efficiency near-vacuum ultraviolet light source with aluminum nitride nanowires monolithically grown on silicon," *Nano Letters*, vol. 15, p. 7006, 2015.
[30] S. Zhao, A. T. Connie, M. H. Dastjerdi, X. H. Kong, Q. Wang, M. Djavid, *et al.*, "Aluminum nitride nanowire light emitting diodes: Breaking the fundamental bottleneck of deep ultraviolet light sources," *Scientific Reports*, vol. 5, p. 8332, 2015.
[31] K. H. Li, X. Liu, Q. Wang, S. Zhao, and Z. Mi, "Ultralow-threshold electrically injected AlGaN nanowire ultraviolet lasers on Si operating at low temperature," *Nature Nanotechnology*, vol. 10, p. 140, 2015.

[32] A. T. Connie, S. Zhao, S. M. Sadaf, I. Shih, Z. Mi, X. Du, *et al.*, "Optical and electrical properties of Mg-doped AlN nanowires grown by molecular beam epitaxy," *Applied Physics Letters*, vol. 106, p. 213105, 2015.
[33] Q. Wang, S. Zhao, A. T. Connie, I. Shih, Z. Mi, T. Gonzalez, *et al.*, "Optical properties of strain-free AlN nanowires grown by molecular beam epitaxy on Si substrates," *Applied Physics Letters*, vol. 104, p. 223107, 2014.
[34] S. Zhao, B. H. Le, D. P. Liu, X. D. Liu, M. G. Kibria, T. Szkopek, *et al.*, "p-Type InN Nanowires," *Nano Letters*, vol. 13, pp. 5509-13, 2013.
[35] S. Zhao, S. Fathololoumi, K. H. Bevan, D. P. Liu, M. G. Kibria, Q. Li, *et al.*, "Tuning the surface charge properties of epitaxial InN nanowires," *Nano Letters*, vol. 12, pp. 2877-82, 2012.
[36] Z. Zhong, F. Qian, D. Wang, and C. M. Lieber, "Synthesis of p-Type Gallium Nitride Nanowires for Electronic and Photonic Nanodevices," *Nano Letters*, vol. 3, p. 343, 2003.
[37] H. Taketomi, Y. Aoki, Y. Takagi, A. Sugiyama, M. Kuwabara, and H. Yoshida, "Over 1 W record-peak-power operation of a 338 nm AlGaN multiple-quantum-well laser diode on a GaN substrate," *Japanese Journal of Applied Physics*, vol. 55, p. 05FJ05, 2016.
[38] H. Yoshida, Y. Yamashita, M. Kuwabara, and H. Kan, "A 342-nm ultraviolet AlGaN multiple-quantum-well laser diode," *Nature Photonics*, vol. 2, pp. 551-554, 2008.
[39] M. Kneissl, Z. Yang, M. Teepe, C. Knollenberg, O. Schmidt, P. Kiesel, *et al.*, "Ultraviolet semiconductor laser diodes on bulk AlN," *Journal of Applied Physics*, vol. 101, p. 123103, 2007.
[40] J. Tatebayashi, S. Kako, J. Ho, Y. Ota, S. Iwamoto, and Y. Arakawa, "Room-temperature lasing in a single nanowire with quantum dots," *Nature Photonics*, vol. 9, pp. 501-505, 2015.